Diosgenin alleviates the inflammatory damage and insulin resistance in high glucose-induced podocyte cells via the AMPK/SIRT1/NF-κB signaling pathway

HAOYU YUAN, HUACHENG SUI and SAIMEI LI

Department of Endocrinology, The First Clinical College of Guangzhou University of Chinese Medicine, Guangzhou, Guangdong 510405, P.R. China

Received November 29, 2022; Accepted March 22, 2023

DOI: 10.3892/etm.2023.11958

Abstract. Diabetic nephropathy (DN) is the predominant cause of end-stage renal disease globally. Diosgenin (DSG) has been reported to play a protective role in podocyte injury in DN. The present study aimed to explore the role of DSG in DN, as well as its mechanism of action in a high glucose (HG)-induced *in vitro* model of DN in podocytes. Cell viability, apoptosis, inflammatory response and insulin-stimulated glucose uptake were evaluated using Cell Counting Kit-8, TUNEL, ELISA and 2-deoxy-D-glucose assay, respectively. In addition, the expression of AMP-activated protein kinase (AMPK)/sirtuin 1 (SIRT1)/NF-κB signaling-related proteins in podocyte cells was measured using western blotting. The results indicated that DSG enhanced the viability of podocytes after HG exposure, but inhibited inflammatory damage and attenuated insulin resistance. Moreover, DSG induced the activation of the AMPK/SIRT1/NF-κB signaling pathway. Furthermore, treatment with compound C, an inhibitor of AMPK, counteracted the protective effects of DSG on HG-induced podocyte cells. Therefore, DSG may be a potential therapeutic compound for the treatment of diabetic nephropathy.

Introduction

Diabetic nephropathy (DN), a major contributor to end-stage renal disease (ESRD), exhibited an increased morbidity and mortality rate worldwide in the past few years (1,2). DN accounts globally for 35-40% of all new clinical cases that need dialysis therapy. DN features morphological and ultrastructural changes in the kidney, such as glomerular hypertrophy, decreased glomerular filtration and renal fibrosis, which make the pathogenesis of DN complicated and poorly understood (3,4). Podocytes, which are localized at the outer layer of the glomerular basement membrane, are well-differentiated epithelial cells constituting the glomerular filtration barrier (5). Notably, the aberrant structure and function of podocytes are considered a predominant driver of DN progression (6). Therefore, focusing on investigating the molecular mechanisms involved in podocyte injury is pivotal to finding novel therapies against DN.

Diosgenin (DSG), a member of the spirostanol steroidal compound family, is abundant in natural herbal medicinal plants and exhibits various biological activities, including cardiovascular protection (7), anti-inflammatory (8) and anticancer (9) activities. On this basis, DSG has attracted widespread attention and has been widely adopted for the management of several diseases, such as cardiovascular diseases (10), diabetes mellitus (11) and osteoporosis (12). Furthermore, DSG is implicated in the process of DN by protecting against podocyte injury (13,14); therefore, preliminary studies on its mechanism of action may confirm the possible application of DSG in DN therapy.

As a primary sensor of cellular energy status, AMP-activated protein kinase (AMPK) is highly conserved in all eukaryotic species (15). In addition, AMPK inhibits the expression of NF-κB by upregulating sirtuin 1 (SIRT1) expression, thus minimizing the inflammatory reaction (16). Moreover, the AMPK/SIRT1/NF-κB signaling pathway has been indicated to be closely associated with the progression of DN (17). Furthermore, a previous study reported that DSG could activate AMPK, thus suppressing the inflammatory response and ameliorating endothelial dysfunction (18).

More importantly, hyperglycemia is involved in the advancement and progression of DN (19); therefore, high glucose (HG) was utilized in the present study to establish an *in vitro* DN model in podocyte cells. The current study aimed to investigate the efficacy of DSG in an *in vitro* DN podocyte model, as well as explore the relationship between DSG and the AMPK/SIRT1/NF-κB signaling pathway.

Materials and methods

Cell culture and treatment. The human podocyte CIHP-1 cell line (Ximbio) was cultured in RPMI-1640 medium (Thermo

Correspondence to: Dr Saimei Li, Department of Endocrinology, The First Clinical College of Guangzhou University of Chinese Medicine, 12 Airport Road, Guangzhou, Guangdong 510405, P.R. China
E-mail: lsaimei210@163.com

Key words: diosgenin, inflammatory damage, insulin resistance, AMP-activated protein kinase/sirtuin 1/NF-κB, diabetic nephropathy

Fisher Scientific, Inc.) supplemented with 10% fetal bovine serum (FBS; Gibco; Thermo Fisher Scientific, Inc.) and 1% penicillin-streptomycin (Sigma-Aldrich; Merck KGaA) at 37˚C with 5% CO_2. Thereafter, cells were treated with HG (30 mM D-glucose) for 48 h at 37˚C (20). Cells treated with normal glucose (NG; 5 mM D-glucose) for 48 h at 37˚C are referred to the control group. To further investigate the mechanism of DSG (cat. no. ID0350; Beijing Solarbio Science & Technology Co., Ltd.), cells were treated with compound C (CC; 10 μM; cat. no. IB0330; Beijing Solarbio Science & Technology Co., Ltd.) for 2 h at 37˚C (21). Mannitol (30 mmol/l; cat. no. SM8120; Beijing Solarbio Science & Technology Co., Ltd.) was used as osmotic control (20).

Cell Counting Kit-8 (CCK-8) assay. Cell viability was measured using the CCK-8 assay (cat. no. C0037; Beyotime Institute of Biotechnology). CIHP-1 cells were seeded into 96-well plates ($1x10^3$ cells/well) and incubated with different concentrations of DSG (0.1, 1.0 and 10.0 μM) for 24 h at 37˚C. Subsequently, the CCK-8 reagent was added to the cells and incubated for 2 h. Finally, the optical density was measured at 450 nm using a microplate reader (BioTek Instruments, Inc.).

Lactate dehydrogenase (LDH) assay. LDH is a stable cytoplasmic enzyme that is found in all cells, and measuring the activity of cytoplasmic enzymes released by damaged cells is a common method for determining cytotoxicity (22). CIHP-1 cells were cultured into a 96-well plate up to 80-90% confluence. Following the different treatments in the respective groups as aforementioned, the plate was centrifuged at 400 x g for 5 min at 4˚C. LDH assay (cat. no. C0016; Beyotime Institute of Biotechnology) was utilized for the determination of LDH activity according to the manufacturer instructions. A total of 100 μl supernatant was added to 100 μl of cytotoxicity assay reagent in a 96-well measurement plate. The LDH activity was determined using the colorimetric detection of sodium pyruvate reduction. Absorbance was measured at 490 nm using a microplate reader (BioTek Instruments, Inc.).

ELISA. CIHP-1 cells were seeded into a 24-well plate ($5x10^4$ cells/well) and treated as previously indicated. Thereafter, cells were centrifuged at 1,000 x g for 5 min at 4˚C. The supernatant was collected and used for ELISA. Tumor necrosis factor-α (TNF-α; cat. no. PT518; Beyotime Institute of Biotechnology), interleukin-1β (IL-1β; cat. no. PI305; Beyotime Institute of Biotechnology) and interleukin-6 (IL-6; cat. no. PI330; Beyotime Institute of Biotechnology) ELISA kits were used. The levels of the inflammatory cytokines TNF-α, IL-1β and IL-6 were determined by measuring the optical density at 450 nm using a microplate reader (Bio-Rad Laboratories, Inc.).

TUNEL assay. To investigate the effects of DSG on the apoptosis of podocyte cells, a TUNEL assay (cat. no. C1082; Beyotime Institute of Biotechnology) was employed. Briefly, CIHP-1 cells ($2x10^4$ cells/well) seeded into a 24-well plate were fixed with 4% paraformaldehyde for 15 min and permeabilized in 0.25% Triton X-100 for 20 min at room temperature. After rinsing in phosphate-buffered saline (PBS; cat. no. C0221A; Beyotime Institute of Biotechnology) three times, the cells were labeled with TUNEL reagent for 60 min at 37˚C, according to the manufacturer's instructions. DAPI staining solution (1 mg/ml; cat. no. C1002; Beyotime Institute of Biotechnology) was utilized to counterstain the cells at 37˚C for 30 min, which were then mounted in an anti-fade reagent (Beijing Solarbio Science & Technology Co., Ltd.). Finally, the images of TUNEL-positive cells were observed in five fields of view selected at random under a fluorescence microscope.

Western blotting. Total protein was extracted from CIHP-1 cells using RIPA lysis buffer (Beijing Solarbio Science & Technology Co., Ltd.) and then quantified using a bicinchoninic acid protein assay kit (cat. no. P0010S; Beyotime Institute of Biotechnology). Total protein (30 μg/lane) was separated on an 8% gel using SDS-PAGE and then transferred onto a PVDF membrane. After blocking with 5% skimmed milk for 2 h at room temperature, membranes were incubated with primary antibodies against Bcl-2 (1:1,000; cat. no. ab32124; Abcam), Bax (1:1,000; cat. no. ab32503), cleaved caspase-3 (1:500; cat. no. ab32042), caspase-3 (1:5,000; cat. no. ab32351), cleaved caspase-9 (1:1,000; cat. no. ab2324), caspase-9 (1:2,000; cat. no. ab32068), nephrin (1:1,000; cat. no. ab216341), phosphorylated (p)-AMPK (1:1,000; cat. no. ab92701), AMPK (1:1,000; cat. no. ab32047), SIRT1 (1:1,000; cat. no. ab189494), NF-κB (1:1,000 cat. no. ab16502) and GAPDH (1:2,500 cat. no. ab9485) (all from Abcam) at 4˚C overnight. On the following day, membranes were incubated with HRP-conjugated secondary antibody (1:2,000; cat. no. ab6721; Abcam) at room temperature for 2 h. Protein bands were visualized using the Immobilon Western Chemiluminescent HRP substrate (cat. no. WBKLS0500; EMD Millipore) and quantified using Image-Pro Plus software (version 6.0; Media Cybernetics, Inc.).

Glucose uptake evaluation. CIHP-1 cells ($5x10^5$) were washed with PBS and incubated in RPMI-1640 medium without serum for 2 h at 37˚C. Subsequently, cells were rinsed in pre-warmed Krebs-Ringer phosphate solution (Sigma-Aldrich; Merck KGaA) containing 2% FBS for 30 min at 37˚C. After being treated with 500 nM insulin (Sigma-Aldrich; Merck KGaA) for 20 min at 37˚C, cells were further incubated with $^{[3H]}$2-deoxy-D-glucose (2-DOG; 50 μmol/l; Sigma-Aldrich: Merck KgaA) (23) for 20 min at 37˚C. Subsequently, ice-cold PBS buffer containing cytochalasin B (10 μmol/l; cat. no. C8080; Beijing Solarbio Science & Technology Co., Ltd.) was added to block the non-specific uptake for 5 min at 37˚C. Finally, the concentration of 2-deoxy-D-glucose-6-phosphate (2-DG6P) was measured at 450 nm using a microplate reader (BioTek Instruments, Inc.).

Reverse transcription-quantitative (RT-q)PCR. Total RNA from CIHP-1 cells seeded into a 6-well plate ($6x10^4$ cells/well) was extracted using TRIzol® reagent (Thermo Fisher Scientific, Inc.). Total RNA was reverse transcribed into cDNA using the PrimerScript reverse transcriptase (Takara Biotechnology Co., Ltd.) according to the manufacturer's protocol. qPCR analysis was performed on a 7500 Real-Time PCR System (Applied Biosystems; Thermo Fisher Scientific, Inc.) using SYBR green Premix Ex Taq II (Qiagen GmbH), according to the manufacturer's protocol. The following thermocycling conditions were

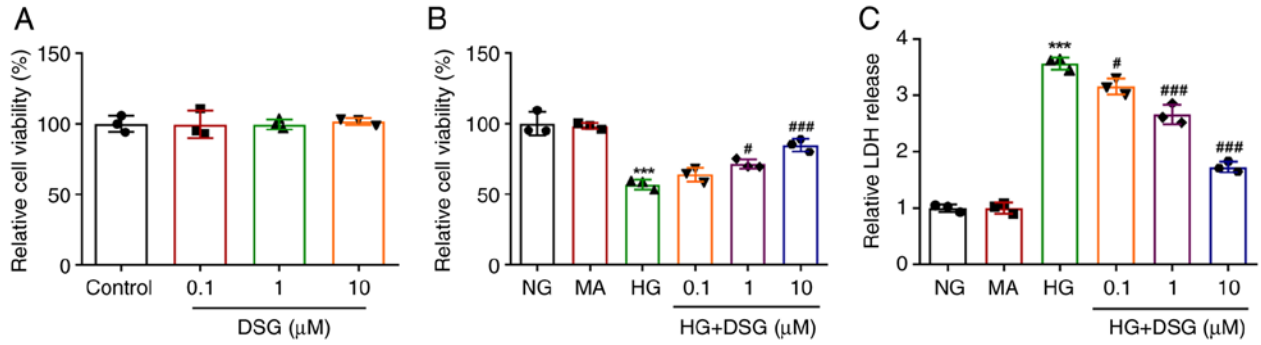

Figure 1. DSG increases the viability of HG-induced podocyte cells. (A) The viability of DSG-treated podocyte cells was measured using the CCK-8 assay. (B) The viability of HG-induced podocyte cells with DSG treatment was detected using the CCK-8 assay. (C) The release of LDH was detected using an LDH assay. ***P<0.001 vs. NG; $^{\#}$P<0.05 and $^{\#\#\#}$P<0.001 vs. HG. DSG, diosgenin; NG, normal glucose; MA, mannitol; HG, high glucose; CCK-8, Cell Counting Kit-8; LDH, lactate dehydrogenase.

used for qPCR: Initial denaturation at 95˚C for 5 min; followed by 40 cycles of denaturation at 95˚C for 45 sec, annealing at 50˚C for 45 sec and elongation at 72˚C for 45 sec; and a final extension step at 72˚C for 10 min. GAPDH was used as an internal reference gene and the relative gene expression was determined using the $2^{-\Delta\Delta Cq}$ method (24). The following primer pairs were used for qPCR: Nephrin forward, 5'-CTGCCT GAAAACCTGACGGT-3' and reverse, 5'-GACCTGGCACTC ATACTCCG-3'; and GAPDH forward, 5'-TGTGGGCATCAA TGGATTTGG-3' and reverse, 5'-ACACCATGTATTCCG GGTCAAT-3'.

Statistical analysis. All data were obtained from three independent repeats and presented as the mean ± standard deviation. The data analysis was performed using GraphPad Prism 8.0 software (GraphPad Software; Dotmatics). Normal distribution and variance heterogeneity were confirmed using the Shapiro-Wilk and Brown-Forsythe tests, respectively. The comparisons among multiple groups were performed using one-way ANOVA followed by Tukey's post hoc test. P<0.05 was considered to indicate a statistically significant difference.

Results

DSG enhances the viability of HG-induced podocyte cells. CCK-8 assay was performed to investigate the impact of DSG on the viability of HG-induced podocyte cells. Cell viability of DSG-treated podocyte cells was not different compared with that in the control group (Fig. 1A). Compared with that in the NG group, the viability of podocyte cells was significantly decreased after HG induction; however, the decreased viability in HG-induced podocyte cells was counteracted by DSG treatment in a concentration-dependent manner (Fig. 1B). HG induction increased the release of LDH in comparison with that in the NG group (Fig. 1C). In addition, DSG decreased the release of LDH in HG-induced podocyte cells compared with that in the NG group.

DSG inhibits the inflammatory damage and apoptosis of HG-induced podocyte cells. To explore the effects of DSG on the inflammatory response and apoptosis of HG-induced podocyte cells, ELISA and TUNEL were used to evaluate the expression of inflammatory cytokines, as well as the cell apoptosis levels. The levels of TNF-α, IL-6 and IL-1β were significantly increased in HG-induced podocyte cells compared with those in the NG group, while they were reduced in HG-induced podocyte cells treated with different concentrations of DSG compared with those in the HG group (Fig. 2A). DSG exhibited inhibitory effects on inflammatory damage in a dose-dependent manner.

Similarly, the apoptosis of podocyte cells was promoted by HG induction compared with that in the NG group (Fig. 2B). However, the increase in apoptosis of HG-induced podocyte cells was subsequently counteracted by DSG treatment (Fig. 2B). In addition, HG induction downregulated Bcl-2 expression, but upregulated the expression of Bax and the ratios of cleaved caspase-3/caspase 3 and cleaved caspase-9/caspase-9 compared with those in the NG group, while DSG treatment reversed the effect of HG induction on the level of these proteins (Fig. 2C). The aforementioned results suggested that DSG inhibited the inflammatory damage and apoptosis of HG-induced renal podocyte cells.

DSG attenuates the insulin resistance (IR) of HG-induced podocyte cells. To clarify the impact of DSG on IR in HG-induced podocyte cells, a 2-DOG assay was performed to assess insulin-stimulated glucose uptake. The expression of nephrin was also evaluated using RT-qPCR and western blotting. Compared with that in the NC group, 2-DG6P levels were decreased in podocyte cells after HG induction. Nevertheless, the decreased levels of 2-DG6P in HG-induced podocyte cells were gradually recovered by treatment with DSG at several concentrations (HG + 1 μM DSG vs. HG, P=0.005; HG + 10 μM DSG vs. HG, P=0.001) (Fig. 3A). Nephrin is a key regulator of podocyte cell permeability, therefore, the mRNA and protein expression of nephrin was measured via RT-qPCR and western blotting. HG induction reduced the expression of nephrin at both mRNA and protein levels compared with those in the NG group, whereas DSG treatment partially counteracted the effect of HG on the nephrin levels, as shown by the increased mRNA and protein expression of nephrin in HG-induced podocyte cells with DSG treatment compared with that in cells induced with HG (Fig. 3B and C).

DSG participates in the regulation of the AMPK/SIRT1/NF-κB signaling pathway. The p-AMPK/AMPK, SIRT1 and NF-κB

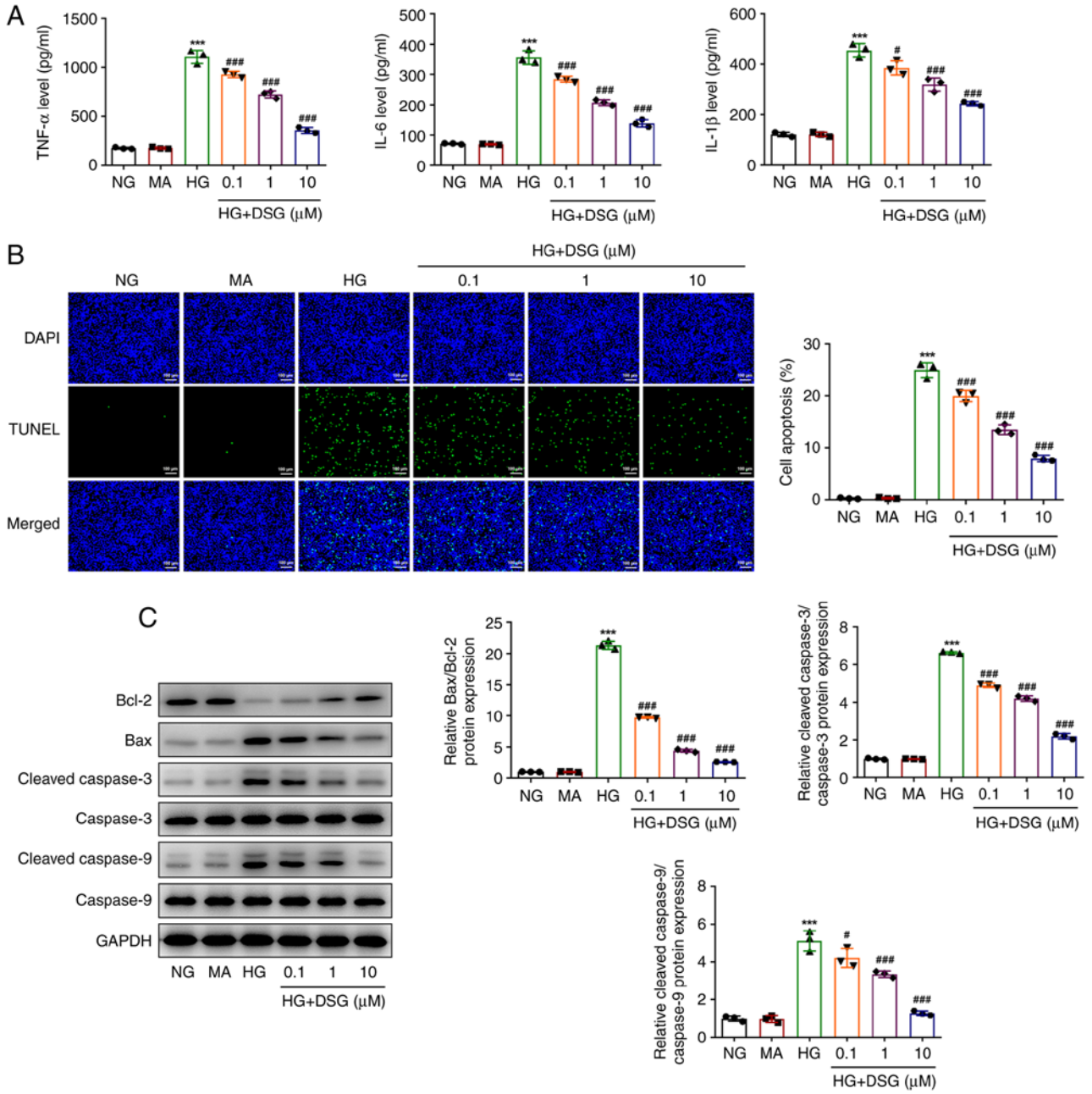

Figure 2. DSG inhibits inflammatory damage in HG-induced podocyte cells. (A) The expression of inflammatory cytokines was measured using ELISA. (B) Apoptosis was detected using TUNEL assay. Scale bar, 100 μm. (C) The expression of apoptosis-related proteins was detected using western blot assays. ***P<0.001 vs. NG; $^{\#}$P<0.05 and $^{\#\#\#}$P<0.001 vs. HG. DSG, diosgenin; NG, normal glucose; MA, mannitol; HG, high glucose.

protein levels were measured to explore the relationship between DSG and the AMPK/SIRT1/NF-κB signaling pathway. HG induction downregulated p-AMPK and SIRT1 expression levels, but upregulated the expression of NF-κB compared with that in the NG group. The effects of HG induction on the expression levels of the aforementioned proteins were reversed after treatment with DSG, suggesting that DSG was involved in the regulation of the AMPK/SIRT1/NF-κB signaling pathway (Fig. 4).

CC reverses the protective effects of DSG on HG-induced podocyte cells. To further investigate the mechanism of DSG, CC, an inhibitor of AMPK, was employed to treat podocyte cells, and subsequently a series of functional experiments were performed. The decreased viability of HG-induced podocyte cells was rescued by DSG treatment; however, CC partially counteracted the effects of DSG, as shown by the reduced viability found in the CC + HG + DSG group compared with that in the HG+DSG group (HG+DSG vs. HG, P=0.002; CC+HG+DSG vs. HG+DSG, P=0.015) (Fig. 5A). Similarly, DSG treatment decreased the LDH release in HG-induced podocyte cells compared with that in the HG group, which was then reversed by CC (Fig. 5B). In addition, compared with that in the NG group, HG increased the expression of inflammatory cytokines, which was then decreased by DSG treatment (Fig. 5C). CC promoted the inflammatory response, as shown by the increase in TNF-α, IL-6 and IL-1β levels compared with those in the

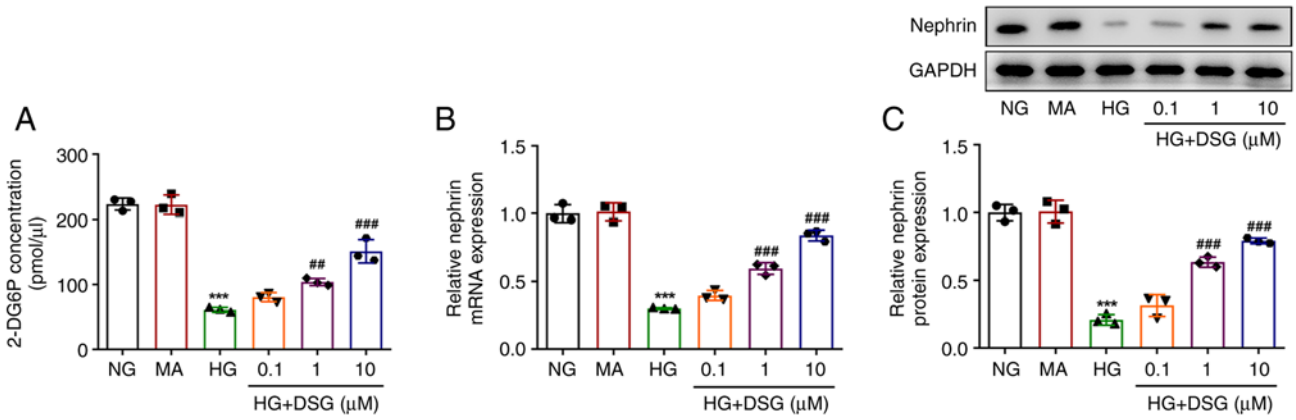

Figure 3. DSG attenuates the insulin resistance of HG-induced podocyte cells. (A) The 2-DG6P concentration was detected using a 2-DOG assay. (B) mRNA and (C) protein expression of nephrin was detected using reverse transcription-quantitative PCR and western blotting, respectively. ***P<0.001 vs. NG; ##P<0.01 and ###P<0.001 vs. HG. DSG, diosgenin; NG, normal glucose; MA, mannitol; HG, high glucose; 2-DG6P, 2-deoxy-D-glucose-6-phosphate.

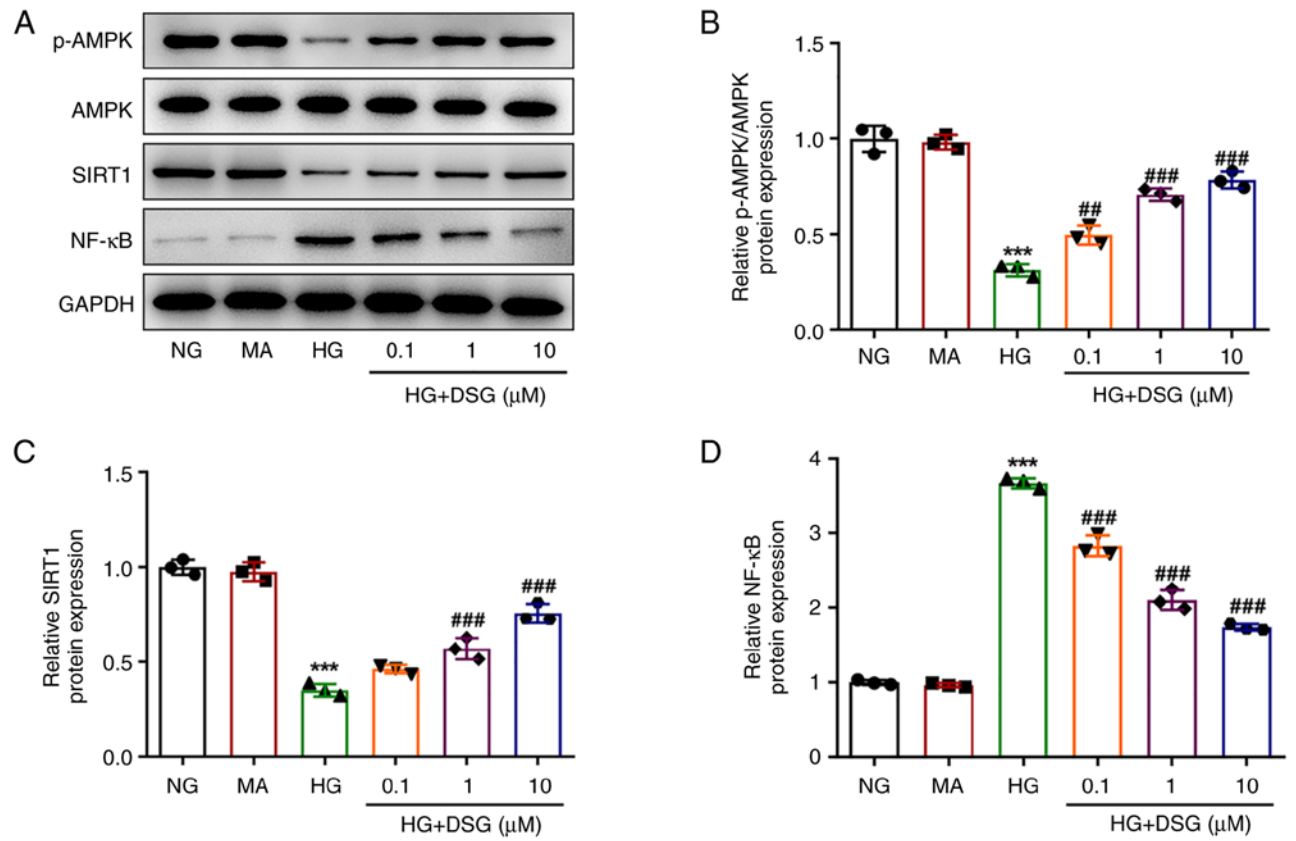

Figure 4. DSG participates in the regulation of the AMPK/SIRT1/NF-κB signaling pathway. (A) The expression of AMPK/SIRT1/NF-κB signaling pathway-related proteins was detected using western blotting. Semi-quantitative expression analysis of (B) phosphorylated-AMPK/AMPK, (C) SIRT1 and (D) NF-κB. ***P<0.001 vs. NG; ##P<0.01 and ###P<0.001 vs. HG. DSG, diosgenin; NG, normal glucose; MA, mannitol; HG, high glucose; AMPK, AMP-activated protein kinase; p-, phosphorylated; SIRT1, sirtuin 1.

HG + DSG group (Fig. 5C). In addition, the inhibitory effects of DSG on the apoptosis of HG-induced podocyte cells were also partially counterbalanced by CC treatment (Fig. 5D). Moreover, the upregulation of Bcl-2, as well as the downregulation of Bax and the cleaved caspase-3/caspase 3 and cleaved caspase-9/caspase-9 ratios caused by DSG in HG-induced podocyte cells compared with the HG group, were attenuated after CC treatment (Fig. 5E). Compared with that in the HG + DSG group, the levels of 2-DG6P were significantly decreased in the CC + HG + DSG (Fig. 6A). In addition, HG induction downregulated nephrin at both mRNA and protein levels compared with the NG group, while DSG treatment increased the nephrin mRNA and protein expression compared with that in the HG group. Finally, the effects of DSG on nephrin were inhibited by CC treatment (Fig. 6B and C). The aforementioned results indicated that CC partially counterbalanced the protective effects of DSG on HG-induced podocyte cells.

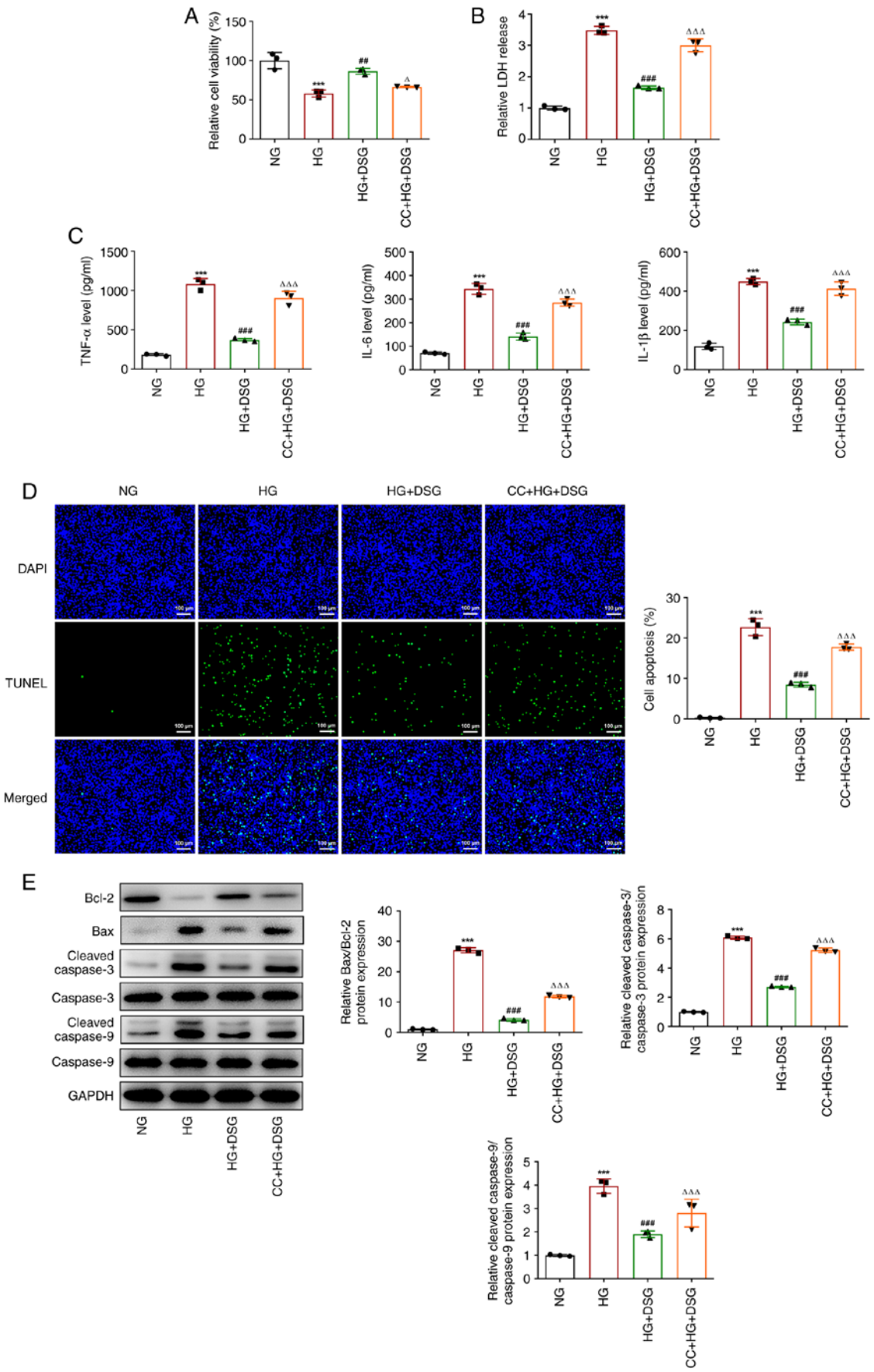

Figure 5. CC reverses the protective effects of DSG on HG-induced podocyte cells. (A) The viability of HG-induced podocyte cells with DSG treatment was measured using Cell Counting Kit-8 assay. (B) The release of LDH was detected using an LDH assay. (C) The expression of inflammatory cytokines was measured using ELISA. (D) Apoptosis was measured using TUNEL assay. Scale bar, 100 μm. (E) The expression of apoptosis-related proteins was measured using western blotting. ***P<0.001 vs. NG; $^{\#\#}$P<0.01 and $^{\#\#\#}$P<0.001 vs. HG; $^{\Delta}$P<0.05 and $^{\Delta\Delta\Delta}$P<0.001 vs. HG + DSG. CC, compound C; DSG, diosgenin; NG, normal glucose; HG, high glucose; LDH, lactate dehydrogenase.

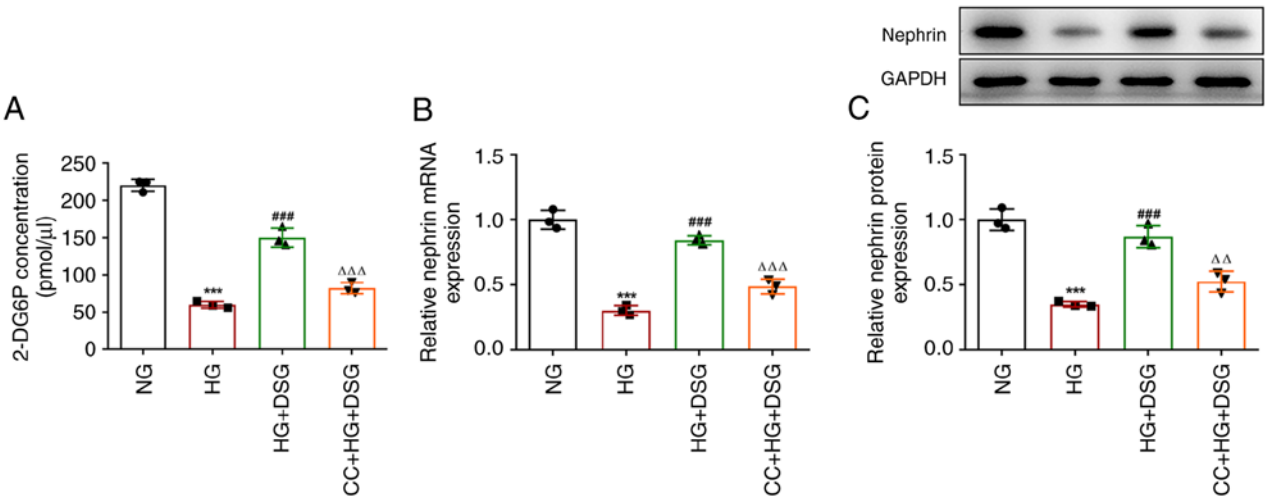

Figure 6. DSG attenuates HG-induced insulin resistance in podocytes via AMP-activated protein kinase signaling. (A) The 2-DG6P levels were measured using a 2-DOG assay. (B) mRNA and (C) protein expression levels of nephrin were measured using reverse transcription-quantitative PCR and western blotting, respectively. ***P<0.001 vs. NG; $^{###}$P<0.001 vs. HG, ^{ΔΔ}P<0.01 and ^{ΔΔΔ}P<0.001 vs. HG + DSG. DSG, diosgenin; NG, normal glucose; HG, high glucose; 2-DG6P, 2-deoxy-D-glucose-6-phosphate.

Discussion

In the present study, HG was used to establish an *in vitro* DN model in podocyte cells. The present results showed that DSG increased cell viability while relieving the inflammatory response, apoptosis and IR of HG-induced podocyte cells in a concentration-dependent manner. In addition, DSG was involved in the regulation of the AMPK/SIRT1/NF-κB signaling pathway, and the AMPK inhibitor CC partially abolished the protective effects of DSG.

As a natural steroidal saponin, DSG is extracted from certain medicinal plants or vegetables, such as fenugreek and yam, and has various pharmacological actions (25). Previous studies have highlighted the beneficial effect of DSG on DN by ameliorating podocyte injury (13,14). In the current study, different concentrations of DSG did not affect the viability of podocyte cells. On the other hand, DSG increased cell viability while suppressing LDH release in HG-induced podocyte cells in a dose-dependent manner. It has been reported that inflammation, as a pathogenic mechanism, is involved in glomerular injury, glomerulosclerosis and eventually ESRD (26). Moreover, DSG has been shown to alleviate inflammatory responses in multiple human diseases. For example, DSG diminished the infiltration of inflammatory cells and the serum levels of inflammatory cytokines in a psoriasis mouse model (27). In addition, Du *et al* (28) suggested that DSG could suppress the release of inflammatory factors in alveolar macrophages, thus protecting against silicosis. Moreover, DSG showed protective effects on testicular damage in streptozotocin-induced diabetic rats by inhibiting the inflammatory response (29). Accordingly, the present study found that the increased levels of TNF-α, IL-6 and IL-1β caused by HG induction were decreased after DSG treatment, revealing the inhibitory effects of DSG on the inflammatory damage of HG-induced podocyte cells. Additionally, the exacerbated apoptosis and the decreased Bcl-2 and increased Bax, cleaved caspase-3/caspase-3 and cleaved caspase-9/caspase-9 expression caused by HG in podocytes were attenuated and reversed by DSG treatment.

IR is a pathophysiological state, and results from a progressive decline in insulin responsiveness in peripheral tissues, including skeletal muscle, adipose tissue and liver (30). Previous studies have shown that DSG treatment could regulate IR. For example, DSG could relieve IR in palmitate-treated human umbilical vein endothelial cells (31). In addition, DSG was also indicated to modulate IR by alleviating the metabolic dysregulation of lipid profile in diabetic rats (32). In the present study, DSG attenuated IR in HG-induced podocyte cells, as demonstrated by the increased levels of 2-DG6P concentration and nephrin expression in HG-exposed podocytes following DSG administration compared with HG treatment alone. Therefore, the current findings suggested that DSG could relieve IR in HG-induced podocyte cells.

It has been reported that the activation of AMPK/SIRT could alleviate inflammation, oxidative stress and apoptosis of podocyte cells (15). Moreover, the activity of AMPKα could alleviate podocyte cells from IR in a DN model (33). More importantly, Ran *et al* (34) showed that DSG could regulate the AMPK and NF-κB signaling pathways. In addition, DSG protected against non-alcoholic fatty liver disease through the regulation of the SIRT1/AMPK signaling pathway (35). In the present study, DSG downregulated NF-κB expression, but upregulated the expression of p-AMPK and SIRT1 in HG-induced podocyte cells, suggesting that DSG participated in the regulation of the AMPK/SIRT1/NF-κB signaling pathway. Furthermore, the protective effects of DSG against decreased cell viability and increased inflammatory response, apoptosis and IR in HG-induced podocyte cells were reversed by CC, an inhibitor of AMPK.

In conclusion, DSG treatment protected HG-induced podocyte cells against the increased inflammatory response and IR by regulating the AMPK/SIRT1/NF-κB signaling pathway, indicating that DSG may represent a novel therapy for the treatment of DN. The present study may offer theoretical insights into the development of DN and the pursuit of novel diagnostic and interventional approaches, and lay a favorable foundation for further investigation. However, there are some

limitations in the current study. Firstly, the toxicity of DSG was not investigated. Secondly, the protective role and therapeutic value of DSG in DN need to be further investigated *in vivo*.

Acknowledgements

Not applicable.

Funding

No funding was received.

Availability of data and materials

The datasets used and/or analyzed during the current study are available from the corresponding author on reasonable request.

Authors' contributions

HY, HS and SL conceived and designed the study, and acquired and interpreted the data. HY and HS performed the experiments. HY and SL wrote the manuscript. HY, HS and SL confirm the authenticity of all the raw data. All authors have read and approved the final manuscript.

Ethics approval and consent to participate

Not applicable.

Patient consent for publication

Not applicable.

Competing interests

The authors declare that they have no competing interests.

References

1. Heerspink HJL, Parving HH, Andress DL, Bakris G, Correa-Rotter R, Hou FF, Kitzman DW, Kohan D, Makino H, McMurray JJV, *et al*: Atrasentan and renal events in patients with type 2 diabetes and chronic kidney disease (SONAR): A double-blind, randomised, placebo-controlled trial. Lancet 393: 1937-1947, 2019.
2. Bell S, Fletcher EH, Brady I, Looker HC, Levin D, Joss N, Traynor JP, Metcalfe W, Conway B, Livingstone S, *et al*: End-stage renal disease and survival in people with diabetes: A national database linkage study. QJM 108: 127-134, 2015.
3. Verzola D, Cappuccino L, D'Amato E, Villaggio B, Gianiorio F, Mij M, Simonato A, Viazzi F, Salvidio G and Garibotto F: Enhanced glomerular Toll-like receptor 4 expression and signaling in patients with type 2 diabetic nephropathy and microalbuminuria. Kidney Int 86: 1229-1243, 2014.
4. Rossing P and Persson F: What have we learned so far from the use of sodium-glucose cotransporter 2 inhibitors in clinical practice? Adv Chronic Kidney Dis 28: 290-297, 2021.
5. Zhu X, Tang L, Mao J, Hameed Y, Zhang J, Li N, Wu D, Huang Y and Li C: Decoding the Mechanism behind the pathogenesis of the focal segmental glomerulosclerosis. Comput Math Methods Med 2022: 1941038, 2022.
6. Tung CW, Hsu YC, Shih YH, Chang PJ and Lin CL: Glomerular mesangial cell and podocyte injuries in diabetic nephropathy. Nephrology (Carlton) 23 (Suppl 4): S32-S37, 2018.
7. Pi WX, Feng XP, Ye LH and Cai BC: Combination of morroniside and diosgenin prevents high glucose-induced cardiomyocytes apoptosis. Molecules 22: 163, 2017.
8. Yang WS, Moon SY, Lee MJ, Lee EK and Park SK: Diosgenin, an activator of 1,25D3-MARRS receptor/ERp57, attenuates the effects of TNF-α by causing ADAM10-dependent ectodomain shedding of TNF receptor 1. Cell Physiol Biochem 43: 2434-2445, 2017.
9. Long C, Chen J, Zhou H, Jiang T, Fang X, Hou D, Liu P and Duan H: Diosgenin exerts its tumor suppressive function via inhibition of Cdc20 in osteosarcoma cells. Cell Cycle 18: 346-358, 2019.
10. Kalailingam P, Kannaian B, Tamilmani E and Kaliaperumal R: Efficacy of natural diosgenin on cardiovascular risk, insulin secretion, and beta cells in streptozotocin (STZ)-induced diabetic rats. Phytomedicine 21: 1154-1161, 2014.
11. Hua S, Li Y, Su L and Liu X: Diosgenin ameliorates gestational diabetes through inhibition of sterol regulatory element-binding protein-1. Biomed Pharmacother 84: 1460-1465, 2016.
12. Chiang SS, Chang SP and Pan TM: Osteoprotective effect of Monascus-fermented dioscorea in ovariectomized rat model of postmenopausal osteoporosis. J Agric Food Chem 59: 9150-9157, 2011.
13. Gan Q, Wang J, Hu J, Lou G, Xiong H, Peng C, Zheng S and Huang Q: The role of diosgenin in diabetes and diabetic complications. J Steroid Biochem Mol Biol 198: 105575, 2020.
14. Wang Z, Wu Q, Wang H, Gao Y, Nie K, Tang Y, Su H, Hu M, Gong J, Fang K and Dong H: Diosgenin protects against podocyte injury in early phase of diabetic nephropathy through regulating SIRT6. Phytomedicine 104: 154276, 2022.
15. Xue W, Mao J, Chen Q, Ling W and Sun Y: Mogroside IIIE alleviates high glucose-induced inflammation, oxidative stress and apoptosis of podocytes by the activation of AMPK/SIRT1 signaling pathway. Diabetes Metab Syndr Obes 13: 3821-3830, 2020.
16. Chen B, Li J and Zhu H: AMP-activated protein kinase attenuates oxLDL uptake in macrophages through PP2A/NF-κB/LOX-1 pathway. Vascul Pharmacol 85: 1-10, 2016.
17. Li F, Chen Y, Li Y, Huang M and Zhao W: Geniposide alleviates diabetic nephropathy of mice through AMPK/SIRT1/NF-kappaB pathway. Eur J Pharmacol 886: 173449, 2020.
18. Chen Y, Xu X, Zhang Y, Liu K, Huang F, Liu B and Kou J: Diosgenin regulates adipokine expression in perivascular adipose tissue and ameliorates endothelial dysfunction via regulation of AMPK. J Steroid Biochem Mol Biol 155: 155-165, 2016.
19. Samsu N: Diabetic nephropathy: Challenges in pathogenesis, diagnosis, and treatment. Biomed Res Int 2021: 1497449, 2021.
20. Li F, Dai B and Ni X: Long non-coding RNA cancer susceptibility candidate 2 (CASC2) alleviates the high glucose-induced injury of CIHP-1 cells via regulating miR-9-5p/PPARγ axis in diabetes nephropathy. Diabetol Metab Syndr 12: 68, 2020.
21. Yang F, Qin Y, Wang Y, Meng S, Xian H, Che H, Lv J, Li Y, Yu Y, Bai Y and Wang L: Metformin Inhibits the NLRP3 inflammasome via AMPK/mTOR-dependent effects in diabetic cardiomyopathy. Int J Biol Sci 15: 1010-1019, 2019.
22. Kumar P, Nagarajan A and Uchil PD: Analysis of cell viability by the lactate dehydrogenase assay. Cold Spring Harb Protoc 2018: doi: 10.1101/pdb.prot095497, 2018.
23. Zhan X, Yan C, Chen Y, Wei X, Xiao J, Deng L, Yang Y, Qiu P and Chen Q: Celastrol antagonizes high glucose-evoked podocyte injury, inflammation and insulin resistance by restoring the HO-1-mediated autophagy pathway. Mol Immunol 104: 61-68, 2018.
24. Li Y, Li Y, Yang T and Wang M: Dioscin attenuates oxLDL uptake and the inflammatory reaction of dendritic cells under high glucose conditions by blocking p38 MAPK. Mol Med Rep 21: 304-310, 2020.
25. Livak KJ and Schmittgen TD: Analysis of relative gene expression data using real-time quantitative PCR and the 2(-Delta Delta C(T)) method. Methods 25: 402-408, 2001.
26. Li G, Huang D, Li N, Ritter JK and Li PL: Regulation of TRPML1 channel activity and inflammatory exosome release by endogenously produced reactive oxygen species in mouse podocytes. Redox Biol 43: 102013, 2021.
27. Wu S, Zhao M, Sun Y, Xie M, Le K, Xu M and Huang C: The potential of Diosgenin in treating psoriasis: Studies from HaCaT keratinocytes and imiquimod-induced murine model. Life Sci 241: 117115, 2020.
28. Du S, Li C, Lu Y, Lei X, Zhang Y, Li S, Liu F, Chen Y, Weng D and Chen J: Dioscin alleviates crystalline silica-induced pulmonary inflammation and fibrosis through promoting alveolar macrophage autophagy. Theranostics 9: 1878-1892, 2019.
29. Khosravi Z, Sedaghat R, Baluchnejadmojarad T and Roghani M: Diosgenin ameliorates testicular damage in streptozotocin-diabetic rats through attenuation of apoptosis, oxidative stress, and inflammation. Int Immunopharmacol 70: 37-46, 2019.

30. Opazo-Rios L, Mas S, Marin-Royo G, Mezzano S, Gómez-Guerrero C, Moreno JA and Egido J: Lipotoxicity and diabetic nephropathy: Novel mechanistic insights and therapeutic opportunities. Int J Mol Sci 21: 2632, 2020.
31. Liu K, Zhao W, Gao X, Huang F, Kou J and Liu B: Diosgenin ameliorates palmitate-induced endothelial dysfunction and insulin resistance via blocking IKKβ and IRS-1 pathways. Atherosclerosis 223: 350-358, 2012.
32. Naidu PB, Ponmurugan P, Begum MS, Mohan K, Meriga B, RavindarNaik R and Saravanan G: Diosgenin reorganises hyperglycaemia and distorted tissue lipid profile in high-fat diet-streptozotocin-induced diabetic rats. J Sci Food Agric 95: 3177-3182, 2015.
33. Lu J, Chen PP, Zhang JX, Li XQ, Wang GH, Yuan BY, Huang SJ, Liu XQ, Jiang TT, Wang MY, *et al*: GPR43 deficiency protects against podocyte insulin resistance in diabetic nephropathy through the restoration of AMPKalpha activity. Theranostics 11: 4728-4742, 2021.
34. Ran X, Yan Z, Yang Y, Hu G, Liu J, Hou S, Guo W, Kan X and Fu S: Dioscin improves pyroptosis in LPS-induced mice mastitis by activating AMPK/Nrf2 and inhibiting the NF-kappaB signaling pathway. Oxid Med Cell Longev 2020: 8845521, 2020.
35. Yao H, Tao X, Xu L, Qi Y, Yin L, Han X, Xu Y, Zheng L and Peng J: Dioscin alleviates non-alcoholic fatty liver disease through adjusting lipid metabolism via SIRT1/AMPK signaling pathway. Pharmacol Res 131: 51-60, 2018.